arXiv:1109.1375v1 [hep-ph] 7 Sep 2011

Effect of the analytic and "frozen" coupling constants in QCD up to NNLO from DIS data

A.V. Kotikov, V.G. Krivokhizhin, and B.G. Shaikhatdenov
Joint Institute for Nuclear Research, Russia

February 25, 2024

Abstract

We give a short review of our recent analysis [1] of the deep inelastic scattering data (provided by BCDMS, SLAC, NMC) on F_2 structure function in the non-singlet approximation with up to next-to-next-to-leading-order accuracy and analytic and frozen modifications of the strong coupling constant featuring no unphysical singularity (the Landau pole). Improvement of agreement between theory and experiment, with respect to the case of the standard perturbative definition of α_s considered recently in [2], was observed.

1 Introduction

At present an accuracy of the data on the deep inelastic scattering (DIS) structure functions (SFs) makes it possible to study separately the Q^2-dependence of logarithmic QCD-inspired corrections and those of power-like (non-perturbative) nature (see for instance [3] and references therein). A part of the power corrections may be responsible for the deviation of the "physical" strong coupling constant from the standard $\overline{\rm MS}$ one. Similar effect was observed recently [4] in the region of small x. In a sense, the study done in [1] is the extension of the analysis [4] to the region of the intermediate and large x values.

In the present paper we show the results of our recent analyse [1] of of DIS SF $F_2(x,Q^2)$ with SLAC, NMC and BCDMS experimental data involved [6]–[8] at NNLO of massless perturbative QCD. This has become possible thanks to the results on both the $\alpha_s^3(Q^2)$ corrections

to the splitting functions (the anomalous dimensions of Wilson operators) [9] and the corresponding expressions of the complete three-loop coefficient functions for the structure functions F_2 and F_L [10]. [1]

As in our previous paper the function $F_2(x,Q^2)$ is represented as a sum of the leading twist $F_2^{pQCD}(x,Q^2)$ and the twist four terms:

$$F_2(x,Q^2) = F_2^{pQCD}(x,Q^2)\left(1+\frac{\tilde{h}_4(x)}{Q^2}\right). \qquad (1)$$

As is known there are at least two ways to perform QCD analysis over DIS data: the first one (see e.g. [13, 14]) deals with Dokshitzer-Gribov-Lipatov-Altarelli-Parisi (DGLAP) integro-differential equations [15] and let the data be examined directly, whereas the second one involves the SF moments and permits performing an analysis in analytic form as opposed to the former option. In this work we take on the way in-between these two latter, i.e. analysis is carried out over the moments of SF $F_2^k(x,Q^2)$ defined as follows

$$M_n^k(Q^2) = \int_0^1 x^{n-2}\,F_2^k(x,Q^2)\,dx \quad (k = \text{pQCD, twist2}\ldots) \qquad (2)$$

and then reconstruct SF for each Q^2 by using Jacobi polynomial expansion method [16, 17] (for further details see [5, 18]). The theoretical input can be found in the papers [18, 19].

2 Infrared modifications of the strong coupling constant

Here, we investigate the potential of modifying the strong-coupling constant in the infrared region with the purpose of illuminating the problem related to the Landau singularity in QCD.

Specifically, we consider two modifications, which effectively increase the argument of the strong-coupling constant at small Q^2 values, in accordance with [20].

In the first case, which is more phenomenological, we introduce freezing of the strong-coupling constant by changing its argument as $Q^2 \to Q^2 + M_\rho^2$, where M_ρ is the rho-meson mass [21] (see also [22, 23] and references therein). Thus, in the formulas of the previous section the following replacement is to be done:

$$a_s^{(i)}(Q^2) \to a_s^{(i),\mathrm{fr}}(Q^2) = a_s^{(i)}(Q^2+M_\rho^2) \quad (i=0,1,2), \qquad (3)$$

[1] For the odd n values, the corresponding coefficients can be obtained by using the analytic continuation [11, 12].

where the symbol $i+1$ marks the ith order of perturbation theory.

A second possibility is based on the idea proposed by Shirkov and Solovtsov [24, 25] (see also recent reviews [26] and references therein) regarding the analyticity of the strong coupling constant in the complex Q^2-plane in the form of the Källén-Lehmann spectral representation. This approach leads effectively to additional power Q^2-dependence for the DIS structure functions (see Eq. (A2)).

2.1 Naive case

This modification is in a sense quite similar to the freezing procedure given above (3), i.e. the one- and two-loop coupling constants $\alpha_s^{(0)}(Q^2)$ and $\alpha_s^{(1)}(Q^2)$ are to be replaced as follows:

$$a_s^{(0)}(Q^2) \;\;\to\;\; a_s^{(0),\mathrm{an}}(Q^2) = a_s^{(0)}(Q^2) - \frac{1}{\beta_0}\,\frac{\Lambda_{(0)}^2}{Q^2-\Lambda_{(0)}^2}, \tag{4}$$

$$a_s^{(1)}(Q^2) \;\;\to\;\; a_s^{(1),\mathrm{an}}(Q^2) = a_s^{(1)}(Q^2) - \frac{1}{2\beta_0}\,\frac{\Lambda_{(1)}^2}{Q^2-\Lambda_{(1)}^2} + \dots\,, \tag{5}$$

where the ellipsis stands for cut terms which give negligible contributions in our analysis.

At the one-loop level, the expression for the analytic coupling constant (4) is very simple. However, at higher-loop levels, it has a rather cumbersome structure (see a recent paper [27] and discussions therein). Therefore, it seems to be simpler to use some proper approximations so as to be able to carry out a numeric analysis.

Considering the study [25], in the NLO case the difference between analytic and standard coupling constants can be represented in the form given in (5), which is similar to the LO one with the additional coefficient equal to 1/2. Note that numerically this NLO term is quite analogous to the LO one, since $\Lambda_{(0)} \ll \Lambda_{(1)}$ (see, for example, [28]).

Following the logic expounded in [23], where it was shown that at the NNLO level the effective LO $\Lambda_{(0)}^{eff}$ can approximately be taken to be

$$\Lambda_{(0)}^{eff} = (2\pi^2)^{\frac{-\beta_1}{2\beta_0^2}}\,\Lambda \sim \frac{1}{2}\Lambda\,, \quad \Lambda \equiv \Lambda_{(2)} \tag{6}$$

we can apply a simple analytic form in the NNLO as follows [2]

$$a_s(Q^2) \to a_s^{\rm an}(Q^2) = a_s(Q^2) - \frac{1}{4\beta_0}\,\frac{\Lambda^2}{Q^2-\Lambda^2} + \dots\,, \quad a_s \equiv a_s^{(2)}\,. \quad (7)$$

Thus, we propose to use this last expression in the NNLO approximation.

In a sense, the replacement quoted in (4), (5) and (7) is a naive way of doing "analytization"; we apply the latter procedure to the coupling constant itself without considering its actual function. Nonetheless, this procedure has already been successfully applied in [22, 4] for analyzing the DIS structure functions at small x values. [3]

With this motivation we would like to investigate its effect in the present study as well. Here it will be referred to as a procedure of the *naive "analytization"*.

2.2 Transition to the canonical form

To accomplish the procedure of "analytization" more accurately [4], it is convenient for the moment $M_n^{NS}(Q^2)$ to be represented in the following form (see [19] and discussions therein)

$$M_n^{NS}(Q^2) = M_n^{NS}(Q_0^2)\cdot\left[\mu_n^{NS}(Q^2,Q_0^2)\right]^{\frac{\gamma_{NS}^{(0)}(n)}{2\beta_0}} \quad (8)$$

where the new "moment" $\mu_n^{NS}(Q^2)$ starts with $a_s(Q^2)$ (see [1]).

The procedure (8) has already been used in [30, 31], where the Grunberg's effective method [32] has been incorporated into the analyses of DIS structure functions.

Now, the "moment" $\mu_n^{NS}(Q^2)$ has the form close to that obtained for the sum rule, because it begins with the first power of $a_s(Q^2)$. Consequently, the form gets closer to that in the difference between the QCD

[2] To have the poles in (5) and (7) exactly cancelled by those in the perturbative expansions of QCD coupling (see, for example, [2]), we keep $Q^2-\Lambda^2_{(i)}$ $(i=0,1,2)$ in the denominators of the additional terms (i.e. in the last terms of (5) and (7)) and, therefore, above LO we will have additional terms coinciding with those in the LO case (with the corresponding replacements $\Lambda_0 \to \Lambda_1$ and $\Lambda_0 \to \Lambda$) multiplied by the additional factor $1/(2i)$.

[3] The results obtained in [4] show that naive analytization as well as freezing of the coupling constant (3) leads to the strong improvement of the agreement with experimental data for the structure function F_2 and its slope at small x values in the double asymptotic scaling regime (see [29] and references therein). Moreover, these results are very similar to the ones [28] obtained in the framework of the infrared renormalon model [3] for HT corrections.

[4] We will call this case an ordinary *analytic perturbation theory (APT)*.

sum rule and its Parton Model value. Following [23], the analytical version of Eq. (8) has the following form [1]

$$\begin{aligned}
\mu^{NS}_{(0),n}(Q^2,Q^2_0) &= \frac{A^{(1)}_1(Q^2)}{A^{(1)}_1(Q^2_0)}\,, \qquad (9)\\
\mu^{NS}_{(1),n}(Q^2,Q^2_0) &= \frac{A^{(2)}_1(Q^2)+A^{(2)}_2(Q^2)\tilde{B}^{(1)}_{NS}(n)}{A^{(2)}_1(Q^2_0)+A^{(2)}_2(Q^2_0)z^{(1)}_{NS}(n)}\,,\\
\mu^{NS}_{n}(Q^2,Q^2_0) &= \frac{A^{(3)}_1(Q^2)+A^{(3)}_2(Q^2)\tilde{B}^{(1)}_{NS}(n)+A^{(3)}_3(Q^2)\tilde{B}^{(2)}_{NS}(n)}{A^{(3)}_1(Q^2_0)+A^{(3)}_2(Q^2_0)z^{(1)}_{NS}(n)+A^{(3)}_3(Q^2_0)z^{(2)}_{NS}(n)}\,,
\end{aligned}$$

where $A^{(i)}_m$ is the "analytized" m-th power of i-loop QCD coupling [24] and the coeffcients $\tilde{B}^{(i)}_{NS}(n)$ and $z^{(i)}_{NS}(n)$ can be found in [1].

Thus, in the APT case the procedure features more complicated functions rather than just the powers of some coupling constant. In the one-loop case the Euclidean functions of analytic perturbation theory (APT) $A^{(1)}_k(Q^2)$ are found to be [25]

$$\begin{aligned}
A^{(1)}_1(Q^2) &= \frac{1}{\beta_0}\left[\frac{1}{L_{(0)}}-\frac{\Lambda^2_{(0)}}{Q^2-\Lambda^2_{(0)}}\right], \quad A^{(1)}_{k+1} = -\frac{1}{k\beta_0}\frac{dA^{(1)}_k}{dL_{(0)}},\\
A^{(1)}_2(Q^2) &= \frac{1}{\beta^2_0}\left[\frac{1}{(L_{(0)})^2}-\frac{\Lambda^2_{(0)}Q^2}{(Q^2-\Lambda^2_{(0)})^2}\right],\\
A^{(1)}_3(Q^2) &= \frac{1}{\beta^3_0}\left[\frac{1}{(L_{(0)})^3}-\frac{\Lambda^2_{(0)}Q^2(Q^2+\Lambda^2_{(0)})}{2(Q^2-\Lambda^2_{(0)})^3}\right], \qquad (10)
\end{aligned}$$

where $L_{(0)}=\ln(Q^2/(\Lambda_{(0)})^2)$, while beyond the LO approximation [25, 23] the transform from standard perturbation theory to the APT is slightly modified to assume the following form:

$$\begin{aligned}
a^{(i)}_s(Q^2)\to A^{(i+1)}_1(Q^2) &= a^{(i)}_s(Q^2)-\frac{1}{2i\beta_0}\frac{\Lambda^2_{(i)}}{Q^2-\Lambda^2_{(i)}}\,, \quad (i=1,2)\\
\left(a^{(i)}_s(Q^2)\right)^2\to A^{(i+1)}_2(Q^2) &= \left(a^{(i)}_s(Q^2)\right)^2-\frac{1}{2i\beta^2_0}\frac{\Lambda^2_{(i)}Q^2}{(Q^2-\Lambda^2_{(i)})^2}\,, \qquad (11)\\
\left(a^{(i)}_s(Q^2)\right)^3\to A^{(i+1)}_3(Q^2) &= \left(a^{(i)}_s(Q^2)\right)^3-\frac{1}{2i\beta^3_0}\frac{\Lambda^2_{(i)}Q^2(Q^2+\Lambda^2_{(i)})}{2(Q^2-\Lambda^2_{(i)})^3}\,,
\end{aligned}$$

where the NLO and NNLO results (for $i=1$ and 2) are only some approximations.

To clear up with the meaning of all these formulas, we would like to note one more time that in the expressions for $A_m^{(i)}(Q^2)$ the lower subscript stands for the power of the coupling constant, while the upper one is related with the order of the approximation considered. Therefore, if the α_s-expansion of some variable starts with the first power, as is the case at hand, then the power of the last term of the expansion coincides with the order of the approximation, i.e. for the last term upper and lower subscripts coincide.

2.3 Fractional analytic perturbation theory

Recently, in a series of papers [33], the analytic continuation (10) has been extended to the noninteger powers of LO $L_{(0)}^{-1}$. In the one-loop case, this so-called fractional APT (FAPT) gives:

$$\frac{1}{L_{(0)}^{\nu}} \to \frac{1}{L_{(0)}^{\nu}} - \frac{\mathrm{Li}_{1-\nu}(e^{-L_{(0)}})}{\Gamma(\nu)}, \tag{12}$$

where

$$\mathrm{Li}_{\nu}(z) = \sum_{m=1}^{\infty} \frac{z^m}{m^{\nu}} \tag{13}$$

is actually the polylogarithm function. [5]

It is clearly seen that by virtue of

$$\mathrm{Li}_0(z) = \frac{z}{1-z},\ \mathrm{Li}_{-N}(z) = \left(z\frac{\mathrm{d}}{\mathrm{d}z}\right)^N \frac{z}{1-z} \ = \ \left(z\frac{\mathrm{d}}{\mathrm{d}z}\right)^N \frac{1}{1-z}\,, \tag{14}$$

all the equations quoted in (10) can be shown to be well reproduced.

Since the product of Γ-functions satisfy

$$\Gamma(\nu)\Gamma(1-\nu) = \frac{\pi}{\sin(\pi\nu)}\,,$$

it is easy to obtain the following representation (see Appendix A in [1]):

$$\frac{\mathrm{Li}_{1-\nu}(z)}{\Gamma(\nu)} \ = \ \frac{z\,\sin(\pi\nu)}{\pi} \int\limits_0^1 \frac{\mathrm{d}\xi}{1-z\xi} \ln^{-\nu}\left(\frac{1}{\xi}\right), \tag{15}$$

that holds for $\Re\mathrm{e}(1-\nu) > 0$ and $\Re\mathrm{e}(\nu) > 0$ (in the case at hand these boil down to $0 < \nu < 1$).

[5] In [33] it was called the Lerch transcendent function.

Then, following the previous section let's recast Eq.(12) in the following fashion:

$$\left(a_s^{(0)}(Q^2)\right)^\nu \to A_\nu^{(1)}(Q^2) \;=\; \left(a_s^{(0)}(Q^2)\right)^\nu - \frac{\mathrm{Li}_{1-\nu}\left(\Lambda^2_{(0)}/Q^2\right)}{\beta_0^\nu \Gamma(\nu)}\,, \quad (16)$$

which reproduces the equations in (10) with $\nu = 1, 2$ and 3, in order.

Above LO, using quite the same arguments as in the previous subsection we have by analogy ($i = 1, 2$):

$$\left(a_s^{(i)}(Q^2)\right)^\nu \to A_\nu^{(i+1)}(Q^2) \;=\; \left(a_s^{(i)}(Q^2)\right)^\nu - \frac{\mathrm{Li}_{1-\nu}\left(\Lambda^2_{(i)}/Q^2\right)}{2i\beta_0^\nu \Gamma(\nu)}\,, (17)$$

which in turn reproduces a set of equations quoted in (11) for $\nu = 1, 2$ and 3, respectively.

Note that the Mellin moments used in this case, contain $\nu = \gamma_{NS}^{(0)}(n)/(2\beta_0) + i$ with $i = 0$ in the LO, $i = 0, 1$ — NLO, and $i = 0, 1, 2$ — NNLO approximations. The argument of the polylogarithm function $\Lambda^2_{(i)}/Q^2$ found in Eqs. (16) and (17) can be expressed through the strong coupling constant (see [1]). Therefore, the power ν lies within the range $0 < \nu < 4$, because $0 < \gamma_{NS}^{(0)}(n)/(2\beta_0) < 2$ for $2 < n < 10$ used in the analyses. The integral representation given in Eq. (15) is correct only for $0 < \nu < 1$, hence the need to extend it to higher values of ν. Omitting details of this latter extension [6] we have ($0 < \delta < 1$)

$$\frac{\mathrm{Li}_{1-N-\delta}(z)}{\Gamma(N+\delta)} \;=\; \left(z\frac{\mathrm{d}}{\mathrm{d}z}\right)^N \left[\frac{z}{\Gamma(N+\delta)\Gamma(1-\delta)} \int\limits_0^1 \frac{\mathrm{d}\xi}{1-z\xi} \ln^{-\delta}\left(\frac{1}{\xi}\right)\right]. \quad (18)$$

To cover an entire range $0 < \nu < 4$, we should consider $N = 0, 1, 2$ and 3. For $N = 0$, Eq. (15) with the corresponding replacement $\nu \to \delta$ can be used. For $N > 0$, it is straightforward to obtain

$$\left(z\frac{\mathrm{d}}{\mathrm{d}z}\right)\frac{z}{1-z\xi} = \frac{z}{(1-z\xi)^2}\,, \qquad \left(z\frac{\mathrm{d}}{\mathrm{d}z}\right)^2\frac{z}{1-z\xi} = \frac{z(1+z\xi)}{(1-z\xi)^3}\,,$$
$$\left(z\frac{\mathrm{d}}{\mathrm{d}z}\right)^3\frac{z}{1-z\xi} \;=\; \frac{z(1+4z\xi+z^2\xi^2)}{(1-z\xi)^4} \quad (19)$$

and make use of the following formulas valid for $0 < \delta < 1$:

$$\frac{\mathrm{Li}_{-\delta}(z)}{\Gamma(1+\delta)} \;=\; \frac{z}{\Gamma(1+\delta)\Gamma(1-\delta)} \int\limits_0^1 \frac{\mathrm{d}\xi \ln^{-\delta}(1/\xi)}{(1-z\xi)^2}, \quad (20)$$

[6] This is done in Appendix A of [1], where $N = 1, 2, 3$. Similar study can be found in the recent paper [34].

$$\frac{\mathrm{Li}_{-1-\delta}(z)}{\Gamma(2+\delta)} = \frac{z}{\Gamma(2+\delta)\Gamma(1-\delta)} \int\limits_0^1 \frac{\mathrm{d}\xi \ln^{-\delta}(1/\xi)}{(1-z\xi)^3} \Big[1+z\xi\Big], \qquad (21)$$

$$\frac{\mathrm{Li}_{-2-\delta}(z)}{\Gamma(3+\delta)} = \frac{z}{\Gamma(3+\delta)\Gamma(1-\delta)} \int\limits_0^1 \frac{\mathrm{d}\xi \ln^{-\delta}(1/\xi)}{(1-z\xi)^4} \Big[1+4z\xi+z^2\xi^2\Big], \qquad (22)$$

i.e. Eqs. (20), (21) and (22) can be used within the ranges $1 < \nu < 2$, $2 < \nu < 3$ and $3 < \nu < 4$, respectively.

3 A fitting procedure

A numeric procedure of fitting the data is described in the previous papers [2, 5]. Here we just recall some aspects of the so-called polynomial expansion method. The latter was first proposed in [35] and further developed in [36]. In these papers the method was based on the Bernstein polynomials and subsequently used to analyze data at NLO [37, 11] and NNLO level [38, 39]. The Jacobi polynomials for that purpose were first proposed and then subsequently developed in [16, 17] and used in [30, 40, 39, 31]

With the QCD expressions for the Mellin moments $M_n^k(Q^2)$ analytically calculated according to the formula in (2), the SF $F_2^k(x,Q^2)$ is reconstructed by using the Jacobi polynomial expansion method:

$$F_2^k(x,Q^2) = x^a(1-x)^b \sum_{n=0}^{N_{max}} \Theta_n^{a,b}(x) \sum_{j=0}^{n} c_j^{(n)}(\alpha,\beta) M_{j+2}^k(Q^2)\,,$$

where $\Theta_n^{a,b}$ are the Jacobi polynomials and a, b are the parameters fitted. A condition put on the latter is the requirement of the error minimization while reconstructing the structure functions.

Since a twist expansion starts to be applicable only above $Q^2 \sim 1$ GeV^2 the cut $Q^2 \geq 1$ GeV^2 on the data is applied throughout.

MINUIT program [41] is used to minimize two variables

$$\chi^2 = \left|\frac{F_2^{exp} - F_2^{teor}}{\Delta F_2^{exp}}\right|^2, \qquad \chi^2_{slope} = \left|\frac{D^{exp} - D^{teor}}{\Delta D^{exp}}\right|^2,$$

where $D = \mathrm{d}\ln F_2/\mathrm{d}\ln\ln Q^2$. The quality of the fits is characterized by χ^2/DOF for the structure function F_2. Analysis is also performed for the SF slope D that serves the purpose of checking the properties of fits (for more details see [2]).

We use free normalizations of the data for different experiments. For a reference set, the most stable deuterium BCDMS data at the value of

the beam initial energy $E_0 = 200$ GeV is used. With the other datasets taken to be a reference one the variation in the results is still negligible. In the case of the fixed normalization for each and all datasets the fits tend to yield a little bit worse χ^2, just as in the previous studies.

4 Results

Since there is no gluons in the nonsinglet approximation the analysis is essentially easier to conduct, with the cut imposed on the Bjorken variable $x \geq 0.25$ where gluon density is believed to be negligible.

Here we conduct separate and combined analyses of SLAC, BCDMS and NMC datasets for hydrogen and deuterium targets. The cut on x is imposed in a combination with those placed on the y variable as follows:

$$\begin{aligned}
y &\geq 0.14 \quad \text{for} \quad 0.3 < x \leq 0.4 \\
y &\geq 0.16 \quad \text{for} \quad 0.4 < x \leq 0.5 \\
y &\geq 0.23 \quad \text{for} \quad 0.5 < x \leq 0.6 \\
y &\geq 0.24 \quad \text{for} \quad 0.6 < x \leq 0.7 \\
y &\geq 0.25 \quad \text{for} \quad 0.7 < x \leq 0.8\,,
\end{aligned}$$

which are meant to cut out those points with large systematic errors. Thus, upon imposing the cuts a complete dataset consists of 327 points in the case of hydrogen target and 288 — deuterium one. The starting point of the QCD evolution is taken to be $Q_0^2 = 90$ GeV^2. This Q_0^2 value is close to the average values of Q^2 spanning the corresponding data. From earlier studies [2, 5] it follows that it is enough to take the maximal value of the number of moments to be accounted for $N_{max} = 8$ [17]; also note that the cut $0.25 \leq x \leq 0.8$ is imposed everywhere.

To reduce the number of parameters, we perform two groups of fits. The first one is dealt within the variable-flavor-number-scheme (VFNS) [2] and the H_2 and D_2 experimental datasets analyzed simultaneously. The results for the second group are obtained within the fixed-flavor-number-scheme (FFNS) with an active number of flavors $n_f = 4$ and the H_2 and D_2 experimental datasets considered separately.

4.1 VFNS case

All the results obtained within our reference VFNS [2] and in the cases of "naive", APT, and "frozen" modifications of α_s are gathered in a set of tables separately for each order of perturbation theory approximation and displayed in Figs. 1–3 separately for all these three cases.

Table 1. *LO values of the twist-four term $\tilde{h}_4(x)$ (with statistic errors given) obtained in the analysis of the combined $H_2 + D_2$ dataset within the VFNS and with various modifications of α_s*

x	Naive analyt. α_s	APT-inspired α_s	Frozen α_s	Standard α_s
0.275	-0.121 ± 0.008	-0.123 ± 0.008	-0.204 ± 0.011	-0.271 ±0.012
0.35	-0.055 ± 0.007	-0.055 ± 0.007	-0.167 ± 0.017	-0.257 ±0.017
0.45	0.119 ± 0.012	0.119 ± 0.012	-0.021 ± 0.031	-0.144 ±0.030
0.55	0.422 ± 0.022	0.422 ± 0.023	0.211 ± 0.053	0.051 ±0.049
0.65	0.870 ± 0.060	0.866 ± 0.059	0.558 ± 0.095	0.364 ±0.088
0.75	1.322 ± 0.117	1.336 ± 0.112	0.917 ± 0.152	0.709 ±0.138
χ^2/DOF	0.93	0.93	0.91	0.94
χ^2_{slope}/DOF	2.30	2.35	2.15	2.60
$\alpha_s(M_Z^2)$	0.1474	0.1474	0.1409	0.1400

Table 2. *NLO values of the twist-four term $\tilde{h}_4(x)$ (with statistic errors given) obtained in the analysis of the combined $H_2 + D_2$ dataset within the VFNS and with various modifications of α_s*

x	Naive analyt. α_s	APT-inspired α_s	Frozen α_s	Standard α_s
0.275	-0.127 ± 0.009	-0.129 ± 0.007	-0.183 ± 0.008	-0.229 ± 0.010
0.35	-0.098 ± 0.007	-0.024 ± 0.009	-0.149 ± 0.010	-0.218 ± 0.016
0.45	0.014 ± 0.012	0.187 ± 0.013	0.010 ± 0.019	-0.084 ± 0.030
0.55	0.172 ± 0.024	0.506 ± 0.019	0.215 ± 0.033	0.098 ± 0.052
0.65	0.339 ± 0.057	0.910 ± 0.045	0.476 ± 0.065	0.356 ± 0.093
0.75	0.478 ± 0.107	1.230 ± 0.090	0.757 ± 0.108	0.648 ± 0.145
χ^2/DOF	0.85	0.84	0.97	1.02
χ^2_{slope}/DOF	0.82	0.78	0.87	1.20
$\alpha_s(M_Z^2)$	0.1275	0.1224	0.1169	0.1152

Table 3. *NNLO values of the twist-four term $\tilde{h}_4(x)$ (with statistic errors given) obtained in the analysis of the combined $H_2 + D_2$ dataset within the VFNS and with various modifications of α_s*

x	Naive analyt. α_s	APT-inspired α_s	Frozen α_s	Standard α_s
0.275	-0.171 ± 0.006	-0.196 ± 0.008	-0.149 ± 0.006	-0.173 ± 0.017
0.35	-0.160 ± 0.008	-0.152 ± 0.012	-0.129 ± 0.013	-0.094 ± 0.020
0.45	-0.044 ± 0.018	0.030 ± 0.022	-0.007 ± 0.031	-0.110 ± 0.015
0.55	0.085 ± 0.033	0.269 ± 0.038	0.116 ± 0.062	-0.086 ± 0.033
0.65	0.221 ± 0.065	0.551 ± 0.074	0.218 ± 0.115	0.085 ± 0.083
0.75	0.304 ± 0.100	0.782 ± 0.116	0.258 ± 0.169	0.158 ± 0.105
χ^2/DOF	0.98	1.02	0.97	0.92
χ^2_{slope}/DOF	1.22	1.17	1.02	1.83
$\alpha_s(M_Z^2)$	0.1151	0.1125	0.1163	0.1159

From Tables 1–3 it is seen that in all the cases considered χ^2/DOF shows good agreement between the experimental data and theoretical predictions for the SF Mellin moments. In LO and NLO cases, the analytic and "frozen" modifications lead to some additional improvement

of fits, namely, χ^2/DOF in these cases is less than that in the standard case.

Since the quantity χ^2_{slope}/DOF is inherently linked with the pQCD aspects to be observed in the data it in this respect is very informative, for it strongly varies from one approximation to the other thus indicating if there are any effects incompatible with the Q^2 dependence in each x-bin assumed. It is seen that it, much like the χ^2/DOF quantity, demonstrates similar tendency: in all the cases considered, the analytic and "frozen" modifications lead to improvement of fits. Certain improvement of the quality of fits is observed at the NLO level. In this approximation even the standard α_s case leads to reasonable agreement for the slopes; furthermore, for all the infrared modifications it is seen that $\chi^2_{slope}/DOF < 1$. In the NNLO approximation the numbers for the slope in the case with a standard α_s are not as good but the infrared modifications (especially the "frozen" one) lead to better agreement between theoretical and experimental results for the former quantity. It is difficult to pin down a reason for such a deterioration of this agreement (in the scheme with a standard α_s) when NNLO corrections are added. Because this effect is absent in the FFNS case (see the following subsection), we suppose that the exact equation for the coupling constant, used here, is somehow in inconsistency with the NNLO expression for the heavy quark thresholds, which is in fact based on certain expansions of the coupling constant at the threshold crossing points (see, for example, [2]). We plan to study this fine effect elsewhere.

The QCD coupling decreases from LO through NNLO, which is in perfect agreement with other studies (see [19] and references therein); it is seen that the frozen modification gives the results closest to those for the standard α_s. In the analytic cases the values of $\alpha_s(M_Z^2)$ are higher in the first two orders of perturbation theory, [7] with the maxima in the difference $\Delta\alpha_s(M_Z^2)$ being 0.0123 and 0.0072 for the naive analytic and APT cases, respectively, observed at NLO. Thus, the differences are substantially greater than the values of the total experimental error $\Delta^{total}\alpha_s(M_Z^2) = 0.0022$, which was obtained in [2] by combining statistical and systematic errors in quadrature.

At the NNLO the APT procedure leads to lower $\alpha_s(M_Z^2)$, though in the naive case the $\alpha_s(M_Z^2)$ value is closer to those obtained for the frozen and standard versions. Nevertheless, all the NNLO $\alpha_s(M_Z^2)$ values, except for the APT case, are in good agreement within statistical errors, which were found to be $\Delta^{stat}\alpha_s(M_Z^2) = 0.0007$ in our previous studies [2]. The APT-inspired QCD coupling constant is compatible

[7] This observation is consistent with earlier studies (see [42] and references therein).

with the rest within the total experimental error.

From Tables 1–3 and, particularly, Figs. 1–3 it is seen that in the cases of analytic and "frozen" coupling constants the twist-four corrections are larger compared to those in the case of a standard perturbative coupling constant, thus confirming the results obtained in [23]. For example, at $x \sim 0.75$ the higher-twist corrections (HTCs) in the standard case are about twice as less that those obtained in the cases of analytic modifications in all orders considered. In the "frozen" case, the HTC values are compatible with those in the standard case within statistical errors. [8]

The difference in the values of HT parameter for the naive analytic and frozen variants becomes moderate at the NLO level unlike the APT case. For the infrared modifications the HT terms are large and in the frozen and APT cases are compatible with the LO ones. A partial explanation of this effect can be found in Appendix A. The "analytization" of the coupling constant generates additional power-like contributions with the opposite sign as compared to the twist-four corrections at large x and, thus, increases effectively the values of HTCs. The analysis in Appendix A is given at the LO level. Above the latter the corresponding results, in accordance with Eqs. (4), (5) and (7), can be estimated by replacing $\Lambda_{(0)} \to \Lambda_{(1)}/2$ in NLO and $\Lambda_{(0)} \to \Lambda/4$ in NNLO in front of the term $\ln(1-x)$ in (A2).

In the NNLO approximation the situation changes drastically. HT terms for all the cases, except for the APT case, are comparable with each other. HTCs in the latter case are still higher but they are also strongly suppressed compared to HTCs in the LO and NLO cases. To some extent, this can be explained by replacing $\Lambda_{(0)} \to \Lambda/4$ in front of $\ln(1-x)$ in (A2), which decreases the influence of the infrared modifications.

Thus, at the NNLO level the twist-four corrections appear to be small for all the cases considered above.

The values for parameters in the parameterizations of the parton distributions for the cases corresponding to different coupling constant modifications are given in Table 4 of [1].

[8] For the results to be discernible, Figs. 1–7 contain statistical errors for the infrared modifications only. The magnitude of the errors is on par in the standard case and is not shown.

4.2 FFNS case

For comparison let's present the values of PDF parameters obtained within the FFNS ($n_f = 4$) in the analyses of the hydrogen and deuterium data for the versions of the strong coupling constant discussed above, with the addition for the case of FAPT-inspired modification of α_s. Here we have no threshold transitions for QCD coupling and PDF Mellin moments and, hence, are able to consider the hydrogen and deuterium datasets separately.

The values for parameters in the parameterizations of the parton distributions for the cases corresponding to different coupling constant modifications are given in Table 5 of [1].

In order to be able to assess the difference among the cases with frozen, FAPT and standard versions for the strong coupling constant let's present the tables with the HT values obtained within FFNS ($n_f = 4$) for the hydrogen data (results obtained for the deuterium data can be found in [1]).

Table 4. *LO values of the twist-four term obtained within the FFNS ($n_f = 4$) and with various modifications of α_s. Only statistical errors are given.*

	FAPT-inspired α_s	Frozen α_s	Standard α_s
x	$\tilde{h}_4(x)$	$\tilde{h}_4(x)$	$\tilde{h}_4(x)$
0.275	-0.221±0.011	-0.183 ± 0.012	-0.235±0.012
0.35	-0.187±0.014	-0.160 ± 0.018	-0.232±0.021
0.45	0.002±0.023	-0.023 ± 0.037	-0.130±0.038
0.55	0.332±0.034	0.189 ± 0.065	0.049±0.065
0.65	1.001±0.063	0.610 ± 0.117	0.455±0.111
0.75	2.031±0.131	1.177 ± 0.207	1.003±0.182
χ^2/DOF	0.98	0.94	0.98
χ^2_{slope}/DOF	1.47	1.25	1.58
$\alpha_s(M_Z^2)$	0.1394	0.1387	0.1376

Table 5. *NLO values of the twist-four term obtained within the FFNS ($n_f = 4$) and with various modifications of α_s.Only statistical errors are given.*

	FAPT-inspired α_s	Frozen α_s	Standard α_s
x	$h_4(x)$	$h_4(x)$	$h_4(x)$ for H_2
0.275	-0.205±0.012	-0.154 ± 0.011	-0.200±0.012
0.35	-0.194±0.017	-0.147 ± 0.016	-0.219±0.019
0.45	-0.067±0.030	-0.058 ± 0.037	-0.169±0.041
0.55	0.160±0.044	0.069 ± 0.067	-0.078±0.072
0.65	0.635±0.071	0.317 ± 0.118	0.153±0.123
0.75	1.512±0.130	0.723 ± 0.204	0.534±0.205
χ^2/DOF	0.91	0.89	0.92
χ^2_{slope}/DOF	1.08	0.92	1.23
$\alpha_s(M_Z^2)$	0.1220 0.1200	0.1192	

Table 6. *NNLO values of the twist-four term obtained within the FFNS ($n_f = 4$) and with various modifications of α_s.Only statistical errors are given.*

	FAPT-inspired α_s	Frozen α_s	Standard α_s
x	$h_4(x)$	$h_4(x)$	$h_4(x)$
0.275	-0.168±0.010	-0.119 ± 0.011	-0.158 ± 0.020
0.35	-0.181±0.015	-0.112 ± 0.010	-0.166 ± 0.021
0.45	-0.130±0.037	-0.049 ± 0.018	-0.156 ± 0.036
0.55	-0.056±0.065	0.007 ± 0.031	-0.157 ± 0.079
0.65	0.126±0.111	0.106 ± 0.058	-0.061 ± 0.127
0.75	0.419±0.178	0.240 ± 0.116	0.049 ± 0.209
χ^2/DOF	0.89	0.87	0.89
χ^2_{slope}/DOF	0.97	0.68	0.97
$\alpha_s(M_Z^2)$	0.1183	0.1180	0.1176

Just like in the previous subsection it is seen from Tables 4–6 that in all the cases at hand, we have good agreement between the experimental data and theoretical predictions. Once again, in all the cases considered, excluding LO FAPT, the analytic and frozen modifications lead to slight improvement of fits, that is χ^2/DOF and χ^2_{slope}/DOF are found to be smaller in these cases than those for the standard α_s, and the QCD coupling constant decreases when we move from LO through NNLO.

Also note that contrary to what was observed in the previous subsection here the quantity χ^2_{slope}/DOF steadily decreases when we proceed step by step from LO to NLO and then to NNLO level. Respectively, here the smaller values of χ^2_{slope}/DOF are observed for the "frozen" case as well.

The values of coupling constants are very similar, especially for the "frozen" and standard versions. In the analytic cases, the central values of $\alpha_s(M_Z^2)$ are little higher, mostly in the first two orders of perturbation theory (see also [42]).

In the NNLO, all the $\alpha_s(M_Z^2)$ values, except for the analytic one, are in good agreement within statistical errors. As earlier, the analytic QCD coupling is in agreement with the rest within the total experimental error.

Similarly to the previous subsection we note in Figs. 4, 5, 6 appreciable difference between HTCs obtained in the standard and analytic cases in the first two orders of perturbation theory. The difference in the cases of a "frozen" and standard α_s is not as large; the values of HT terms are in agreement within statistical errors (see Fig. 7).

In the NNLO, the situation is over again changed considerably. In all the cases of infrared modifications considered, the HTCs are small. Similarly to the previous subsection they are not compatible with zero at $x \sim 0.75$, while the HT terms in standard QCD are compatible with

zero and, at the same time, in agreement with all the cases considered within statistical errors.

Then, at NNLO we can see agreement between standard QCD and its infrared modifications for QCD coupling $\alpha_s(M_Z^2)$, as well as for the respective HTCs (as a rule) within statistical errors.

5 Conclusions

The pattern of separating perturbative QCD and HT corrections may be different in different orders of perturbation theory, as well as in some resummations based on several first orders, and for certain modifications of the strong coupling constant as well. In the present paper, we have shown the results of our recent analysis [1], where we studied the consequences of the infrared modifications of the QCD coupling constant — the so-called "frozen" and "analytized" versions. In the last case three different options were considered:

- a simple modification of the strong coupling constant [24] without rearrangement of a perturbation series;
- an application of the ordinary analytic perturbation theory (see [23]) to the "moments" $\mu_n^{NS}(Q^2)$ given in (8);
- impact of the fractional analytic perturbation theory [33] applied directly to the Mellin moments $M_n^{NS}(Q^2)$.

To test all these modifications, the Jacobi polynomial expansion method developed in [16, 17] was used to perform analysis of Q^2-evolution of the DIS structure function F_2 by fitting all existing to date reliable fixed-target experimental data that satisfy the cut $x \geq 0.25$. To the best of our knowledge, the study [1] is the first application of the FAPT results to the fits of the DIS structure functions.

The main conclusions are as follows. In the first two orders of perturbation theory, the coupling constant $\alpha_s(M_Z^2)$ rises for all versions of the analytic perturbation theory. This observation is in complete agreement with recent studies in [42].

An increase in the central values of $\alpha_s(M_Z^2)$ is smaller in the NNLO approximation, much like in the case of the "frozen" version of α_s. Nevertheless, in all the cases the $\alpha_s(M_Z^2)$ values are in agreement mostly within total experimental errors. For the NNLO case, the results are as a rule compatible between each other within statistical errors. Also, we note that within statistical errors only (in our case $\Delta^{stat}\alpha_s(M_Z^2) = 0.0007$ [2]) all the NNLO results for $\alpha_s(M_Z^2)$ in the FFNS case (see

Table 6) are too compatible with the world average value for the coupling constant presented in the review [43] [9]:

$$\alpha_s(M_Z^2) = 0.1184 \pm 0.0007\,.$$

It is also observed that there is some rise of the twist-four corrections in the first two orders of perturbation theory, particularly for all versions of the analytic one. This observation is in complete agreement with recent studies [23] of the Bjorken sum rules, where it was shown that there is a reduction of higher HT terms, starting with the twist-six ones. Unfortunately, in [1] we were not able to study the twist-four and twist-six corrections simultaneously since their contributions are strongly correlated.

In the NNLO, all the cases of infrared modifications of the QCD coupling feature nonzero although rather small twist-four corrections. Whereas in the case of the standard QCD approach, the HT terms are close to zero at large values of the Bjorken variable x. However, the NNLO HTCs for all the cases considered are compatible between each other within statistical errors.

In principle, the main difference between the cases with a standard QCD coupling constant and its analytic and "frozen" modifications is in the strong suppression of the higher twist corrections in NLO and NNLO orders of perturbation theory, respectively.

What is interesting to look for further in the study is the consideration of the combined nonsinglet and singlet analyses using the DIS experimental data within an entire x region, as well as an application of certain resummation-like Grunberg effective charge methods [32] (as was done in [31] in the NLO approximation) and the "frozen" [21] [10] and analytic [25] versions of the strong coupling constant (see [4, 22, 23] for recent studies in this direction). The effect of $\mathrm{N^3LO}$ corrections would also seem to be important to account for in the subsequent investigations, as well as an extension of the FAPT model results for α_s to the VFNS case.

[9] It should be mentioned that this analysis was carried out over the data coming from the various experiments and in different orders of perturbation theory, i.e. from NLO up to $\mathrm{N^3LO}$.

[10] There are a lot of "frozen" versions of the strong coupling constant (see, for example, the list of references in [22]).

6 Acknowledgments

The work was supported by the RFBR grant No.10-02-01259-a. We are grateful to S.V. Mikhailov, D.B. Stamenov and O.V. Teryaev for useful discussions.

7 Appendix A

Consider the large x asymptotic [44] of SF $F_2(x,Q^2)$ (for simplicity we restrict ourselves to the LO approximation)

$$F_2(x,Q^2) \sim (1-x)^{b(a_s^{(0)}(Q^2))}, \tag{A1}$$

where

$$b\left(a_s^{(0)}(Q^2)\right) = b_0 - \tilde{d}\ln(a_s^{(0)}(Q^2)), \quad \tilde{d} = \frac{16}{3\beta_0},$$

and b_0 is some constant which can be obtained from the quark counting rules [45].

The Q^2-dependent part in the r.h.s. of (A1) can be represented as follows:

$$(1-x)^{-\tilde{d}\ln(a_s^{(0)}(Q^2))} = \left[a_s^{(0)}(Q^2)\right]^{-\tilde{d}\ln(1-x)}.$$

Performing the "analytization" procedure and using (4), we have [11]

$$\left(a_s^{(0)}(Q^2) - \frac{1}{\beta_0}\frac{\Lambda^2_{(0)}}{Q^2-\Lambda^2_{(0)}}\right)^{-\tilde{d}\ln(1-x)}$$
$$\approx \left[a_s^{(0)}(Q^2)\right]^{-\tilde{d}\ln(1-x)}\left[1 + \frac{\tilde{d}\ln(1-x)}{\beta_0 a_s^{(0)}(Q^2)}\frac{\Lambda^2_{(0)}}{Q^2-\Lambda^2_{(0)}}\right]. \tag{A2}$$

From this expression it follows that the power corrections, which were generated by the "analytization" of the coupling constant, have the opposite sign as compared to the twist-four corrections at large x and, moreover, demonstrate a different asymptotic behavior. These corrections (taken with the additional sign "$-$") increase like $\ln(1-x)$ while the twist-four corrections behave like $1/(1-x)$ (see [47] and discussions therein). This difference in sign between these corrections leads to the larger twist-four corrections in the present analysis than those given in [2].

[11] This analysis is carried out at rather large Q^2 values used in the paper. For low Q^2, consideration can be found, for example, in [46].

References

[1] A. V. Kotikov, V. G. Krivokhizhin and B. G. Shaikhatdenov, arXiv:1008.0545 [hep-ph]; Phys.Atom.Nucl. (2011), in press.

[2] B.G. Shaikhatdenov, A.V. Kotikov, V.G. Krivokhizhin, and G. Parente, Phys. Rev. **D81** (2010) 034008.

[3] M. Beneke, Phys. Rept. **317** (1999) 1.

[4] G. Cvetic, A. Y. Illarionov, B. A. Kniehl and A. V. Kotikov, Phys. Lett.**B679** (2009) 350.

[5] V.G. Krivokhizhin, A.V. Kotikov, Yad.Fiz. **68** (2005) 1935 [Phys.Atom.Nucl. **68** (2005) 1873].

[6] SLAC Collab., L.W. Whitlow et al., Phys. Lett. **B282** (1992) 475; L.W. Whitlow, Ph.D. Thesis Standford University, SLAC report 357 (1990).

[7] NMC Collab., M. Arneodo et al., Nucl. Phys. **B483** (1997) 3.

[8] BCDMS Collab., A.C. Benevenuti et al., Phys. Lett. **B223** (1989) 485; Phys. Lett. **B237** (1990) 592; Phys. Lett. **B195** (1987) 91.

[9] J.A.M. Vermaseren, A. Vogt, S. Moch, Nucl.Phys.**B688** (2004) 101; hep-ph/0403192

[10] J.A.M. Vermaseren, A. Vogt, S. Moch, Nucl.Phys.**B724** (2005) 3; hep-ph/0504242

[11] D.I. Kazakov and A.V. Kotikov, Nucl.Phys. **B307** (1988) 791; (E: **345**, 299 (1990)).

[12] A.V. Kotikov and V.N. Velizhanin, hep-ph/0501274; A.V. Kotikov, Phys. Atom. Nucl. **57** (1994) 133. [Yad.Fiz. **57** (1994) 142]

[13] M. Virchaux and A. Milsztajn, Phys. Lett. **B274** (1992) 221.

[14] A.D. Martin, W.J. Stirling, R.S. Thorne, and G. Watt, Phys. Lett. **B652** (2007) 292; A.D. Martin, R.G. Roberts, W.J. Stirling and R.S. Thorne, Eur. Phys. J. **C28** (2003) 455; Eur. Phys. J. **C35** (2004) 325;
P. Jimenez-Delgado and E. Reya, Phys. Rev. **D79** (2009) 074023; M Gluck, C. Pisano and E. Reya, Phys. Rev. **D77** (2008) 074002; M Gluck, P. Jimenez-Delgado and E. Reya, Eur. Phys. J. **C53** (2008) 355;
CTEQ Collab., W.K. Tung, H.Lai, A. Belyaev, J. Pumplin, D. Sturm, and C.-P. Yuan, JHEP **0702** (2007) 053; H.Lai, P.M. Nadolsky, J. Pumplin, D. Sturm, W.K. Tung, and C.-P. Yuan, JHEP

0704 (2007) 089; S. Kretzer, H.L. Lai, F.I. Olness, and W.K. Tung, Phys. Rev. **D69** (2004) 114005;
S.I. Alekhin, JETP Lett. **82** (2005) 628; Phys. Rev. **D68** (2003) 014002; JHEP **0302** (2003) 015; Phys. Lett. **B519** (2001) 57.

[15] V.N. Gribov and L.N. Lipatov, Sov. J. Nucl. Phys. **15** (1972) 438; L.N. Lipatov, Sov. J. Nucl. Phys. **20** (1975) 94;
G. Altarelli and G. Parisi, Nucl. Phys. **B126** (1977) 298;
Yu.L. Dokshitzer, JETP **46** (1977) 641.

[16] G. Parisi and N. Sourlas, Nucl. Phys. **B151** (1979) 421;
I.S. Barker, C.B. Langensiepen and G. Shaw, Nucl. Phys. **B186** (1981) 61; I.S. Barker, B.R. Martin, and G. Shaw, Z. Phys. **C19** (1983) 147; I.S. Barker and B.R. Martin, Z. Phys. **C24** (1984) 255.

[17] V.G. Krivokhizhin, S.P. Kurlovich, V.V. Sanadze, I.A. Savin, A.V. Sidorov and N.B. Skachkov, Z. Phys. **C36** (1987) 51; V.G. Krivokhizhin, S.P. Kurlovich, R. Lednicky, S. Nemechek, V.V. Sanadze, I.A. Savin, A.V. Sidorov and N.B. Skachkov, Z. Phys. **C48** (1990) 347.

[18] V.G. Krivokhizhin, A.V. Kotikov, Phys.Part.Nucl. **40** (2009) 1059.

[19] A. V. Kotikov, Phys. Part. Nucl. **38** (2007) 1 [Erratum-ibid. **38** (2007) 828].

[20] Y. L. Dokshitzer and D. V. Shirkov, Z. Phys. C **67** (1995) 449;
A. V. Kotikov, Phys. Lett. B **338** (1994) 349 [JETP Lett.**59** (1995) 1] .
S. J. Brodsky, V. S. Fadin, V. T. Kim, L. N. Lipatov and G. B. Pivovarov, JETP Lett. **70** (1999) 155.

[21] B. Badelek, J. Kwiecinski, and A. Stasto, Z. Phys. **C74** (1997) 297.

[22] A.V. Kotikov, A.V. Lipatov, and N.P. Zotov, J. Exp. Theor. Phys. **101** (2005) 811 [ZETP **128** (2005) 938].

[23] R.S. Pasechnik, D.V. Shirkov, and O.V. Teryaev, Phys. Rev. **D78** (2008) 071902; R.S. Pasechnik, D.V. Shirkov, O.V. Teryaev, O.P. Solovtsova, and V.L. Khandramai, Phys. Rev. **D81** (2010) 016010; R.S. Pasechnik, J. Soffer, O.V. Teryaev, Phys. Rev. **D82** (2010) 076007.

[24] D.V. Shirkov and I.L. Solovtsov, Phys. Rev. Lett. **79** (1997) 1209.

[25] I. L. Solovtsov and D. V. Shirkov, Theor. Math. Phys. **120** (1999) 1220 [Teor. Mat. Fiz. **120** (1999) 482] [arXiv:hep-ph/9909305].

[26] G. Cvetič and C. Valenzuela, Braz. J. Phys. **38** (2008) 371;
A.P. Bakulev, Phys. Part. Nucl. **40** (2009) 715.

[27] A. V. Nesterenko and C. Simolo, Comput. Phys. Commun. **181** (2010) 1769.

[28] A. Yu. Illarionov, A. V. Kotikov and G. Parente Bermudez, Phys. Part. Nucl. **39** (2008) 307.

[29] A.V. Kotikov and G. Parente, Nucl. Phys. **B549** (1999) 242.

[30] G. Parente, A.V. Kotikov and V.G. Krivokhizhin, Phys. Lett. **B333** (1994) 190;

[31] V.I. Vovk, Z. Phys. **C47** (1990) 57;
A.V. Kotikov, G. Parente and J. Sanchez Guillen, Z. Phys. **C58** (1993) 465.

[32] G. Grunberg, Phys. Lett. **B95** (1980) 70; Phys. Rev. **D29** (1984) 2315.

[33] A. P. Bakulev, S. V. Mikhailov and N. G. Stefanis, Phys. Rev. D **72** (2005) 074014 [Erratum-ibid. D **72** (2005) 119908]; A. P. Bakulev, S. V. Mikhailov and N. G. Stefanis, Phys. Rev. D **75** (2007) 056005. [Erratum-ibid. D **77** (2008) 079901]; JHEP **1006** (2010) 085.

[34] G. Cvetic and A. V. Kotikov, arXiv:1106.4275 [hep-ph].

[35] F.J. Yndurain, Phys. Lett. **B74** (1978) 68.

[36] A. Gonzalez-Arroyo, C. Lopez, Nucl.Phys. **B166** (1980) 429;
A. Gonzalez-Arroyo, C. Lopez, F.J. Yndurain, Nucl.Phys. **B174** (1980) 474.

[37] B. Escobles, M.J. Herrero, C. Lopez, and F.J. Yndurain, Nucl. Phys. **B242** (1984) 329;
D.I. Kazakov and A.V. Kotikov, Sov. J. Nucl. Phys. **46** (1987) 1057 [Yad. Fiz. **46** (1987) 1767].

[38] J. Santiago and F.J. Yndurain, Nucl. Phys. **B563** (1999) 45.

[39] A.L. Kataev, G. Parente and A.V. Sidorov, Phys. Part. Nucl. **34** (2003) 20.

[40] A.L. Kataev, A.V. Kotikov, G. Parente and A.V. Sidorov, Phys. Lett. **B388** (1996) 179; Phys. Lett. **B417** (1998) 374; A.V. Sidorov, Phys. Lett. **B389** (1996) 379; A.L. Kataev, G. Parente and A.V. Sidorov, Nucl. Phys. **B573** (2000) 405.

[41] F. James and M. Ross, "MINUIT", CERN Computer Center Library, D 505, Geneve, 1987.

[42] D. V. Shirkov, Eur. Phys. J. **C22** (2001) 331; K. A. Milton, I. L. Solovtsov, and O. P. Solovtsova, Phys. Rev. **D64** (2001) 016005; Eur. Phys. J. **C14** (2000) 495.

[43] S. Bethke, Eur. Phys. J. Phys. **C64** (2009) 689.

[44] D.I. Gross, Phys. Rev. Lett. **32** (1974) 1071;
D.I. Gross and S.B. Treiman, Phys. Rev. Lett. **32** (1974) 1145.

[45] V.A. Matveev, R.M. Muradian and A.N. Tavkhelidze, Lett. Nuovo Cim. **7** (1973) 719;
S.J. Brodsky and G.R. Farrar, Phys. Rev. Lett. **31** (1973) 1153;
S.J. Brodsky, J. Ellis, E. Gardi, M. Karliner and M.A. Samuel, Phys. Rev. **D56** (1997) 6980.

[46] G. Cvetic, R. Koegerler, and C. Valenzuela, Phys. Rev. **D82** (2010) 114004; J. Phys. **G37** (2010) 075001.

[47] F.J. Yndurain, *Quantum Chromodynamics (An Introduction to the Theory of Quarks and Gluons), Berlin, Springer-Verlag* (1983).

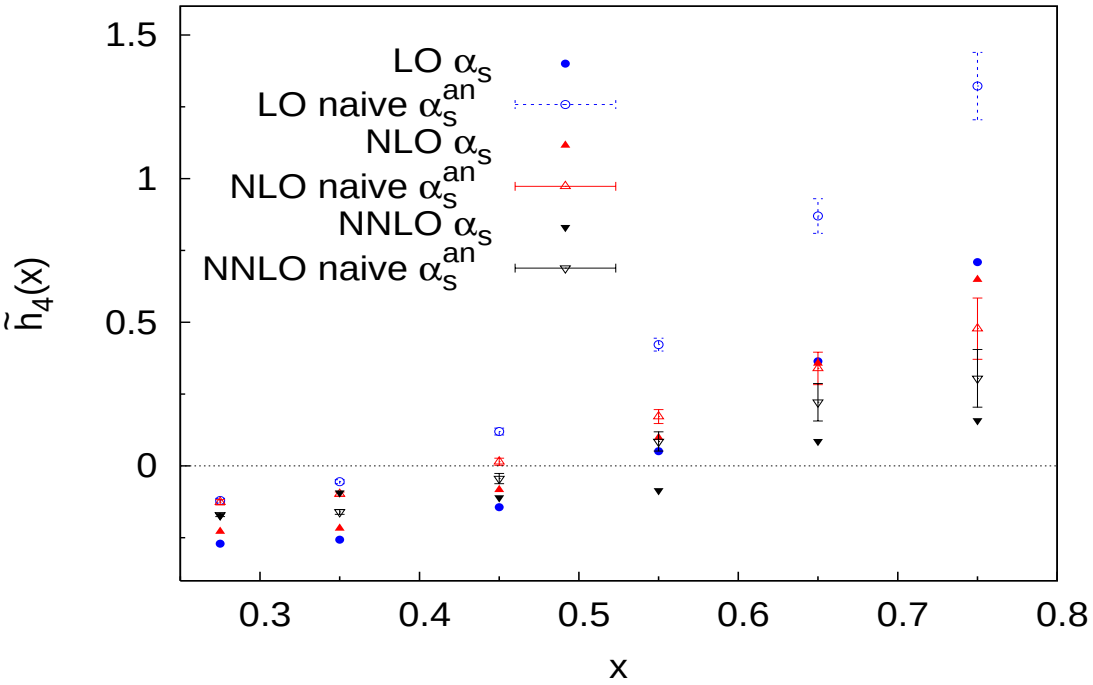


Figure 1: Comparison of the HTC parameter $\tilde{h}_4(x)$ obtained in LO, NLO and NNLO for hydrogen data (the bars stand for statistical errors) between our reference VFNS with a standard perturbative α_s [2] and that with naive analytic α_s.

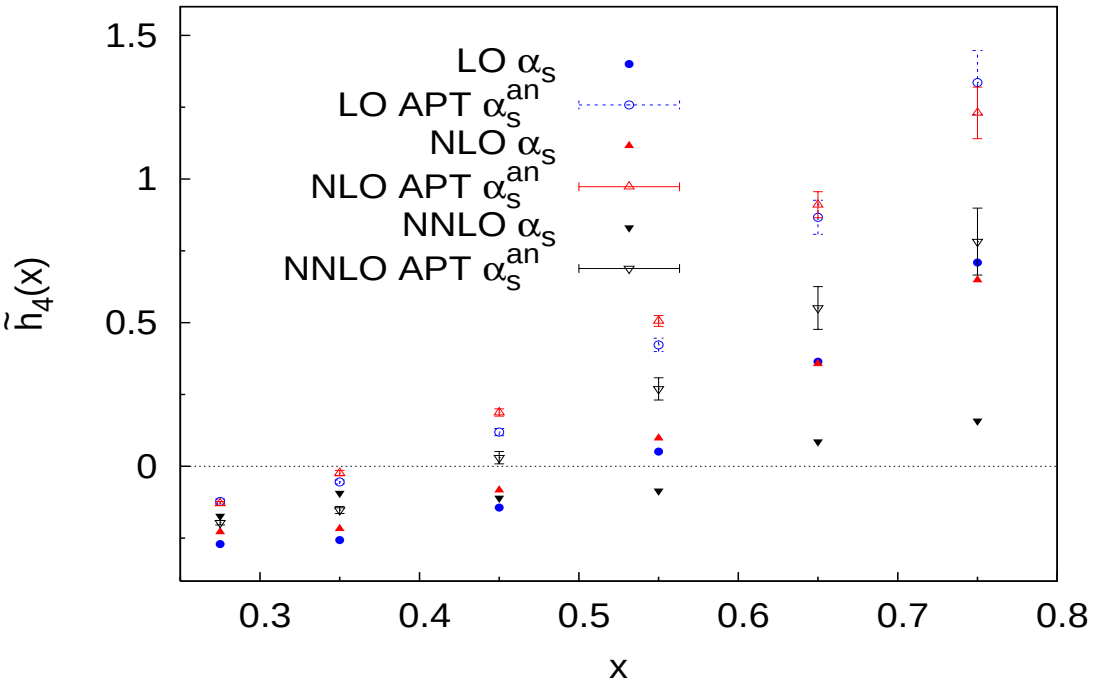


Figure 2: Comparison of the HTC parameter $\tilde{h}_4(x)$ obtained in LO, NLO and NNLO for hydrogen data between a VFNS and that with APT-inspired α_s.

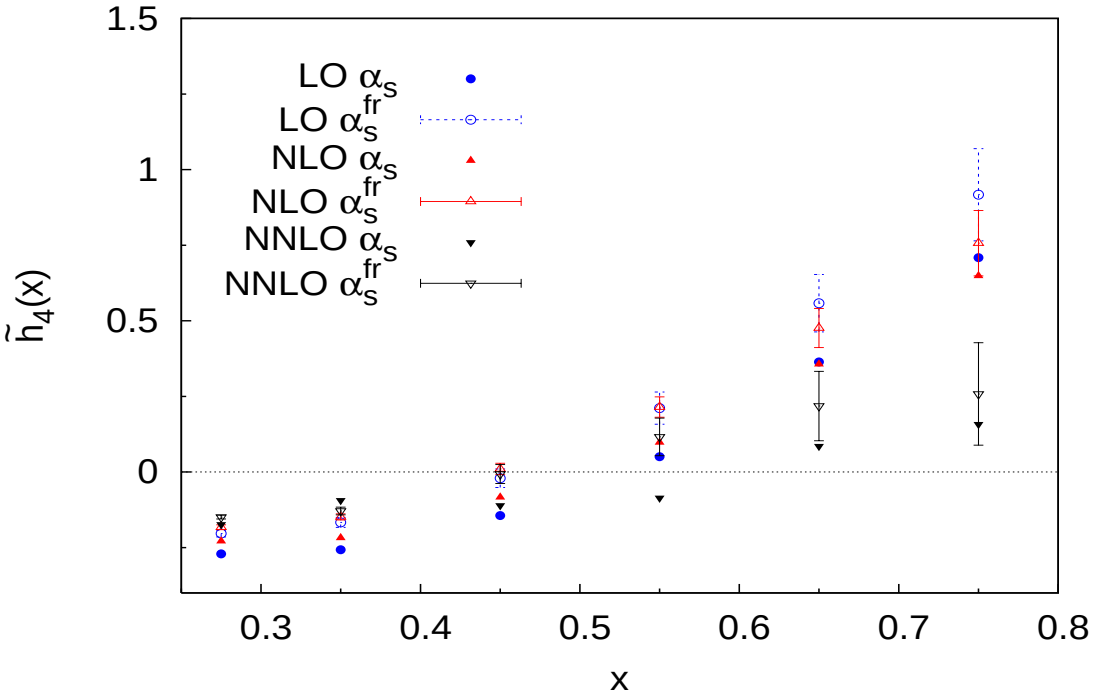


Figure 3: Comparison of the HTC parameter $\tilde{h}_4(x)$ obtained at LO, NLO and NNLO for hydrogen data within a VFNS between the cases with a standard perturbative and "frozen" α_s.

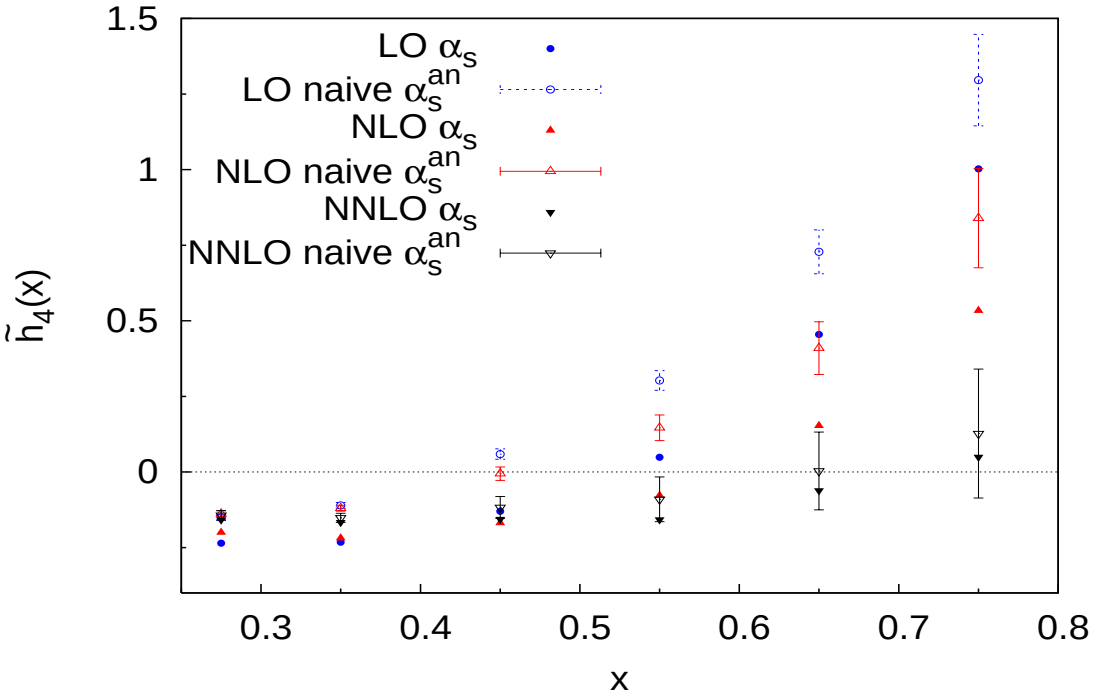


Figure 4: Comparison of the HTC parameter $\tilde{h}_4(x)$ obtained in LO, NLO and NNLO for hydrogen data within a FFNS ($n_f = 4$) between the cases with a standard perturbative and naively analytized α_s.

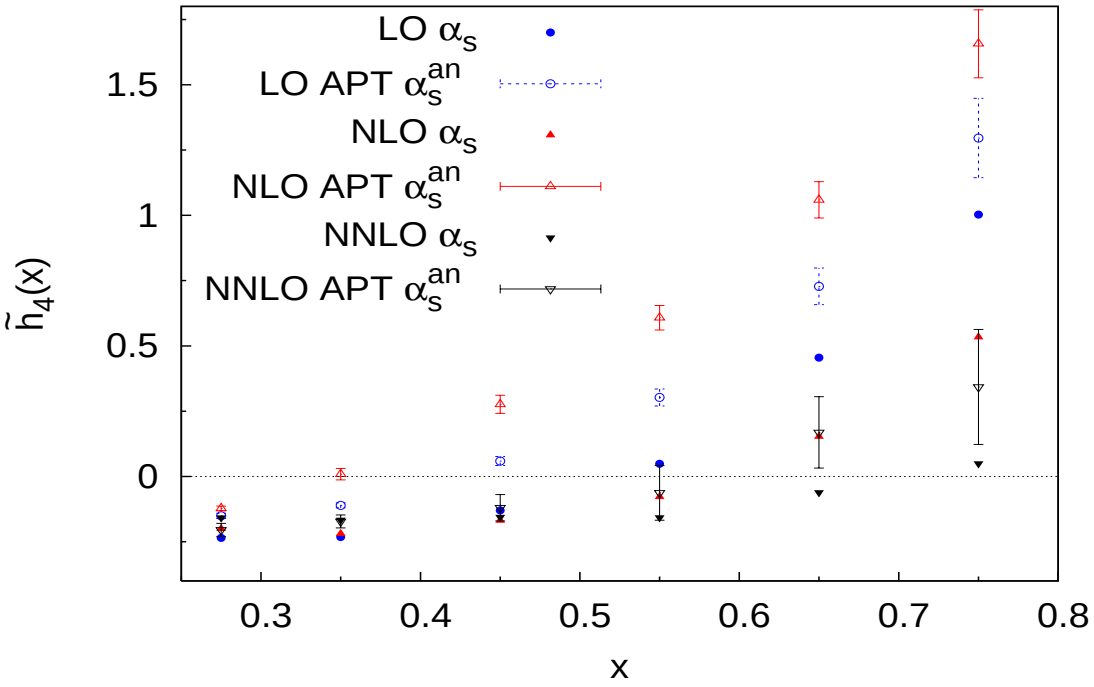


Figure 5: Comparison of the HTC parameter $\tilde{h}_4(x)$ obtained in LO, NLO and NNLO for hydrogen data within a FFNS ($n_f = 4$) between the cases with a standard perturbative and APT-inspired α_s.

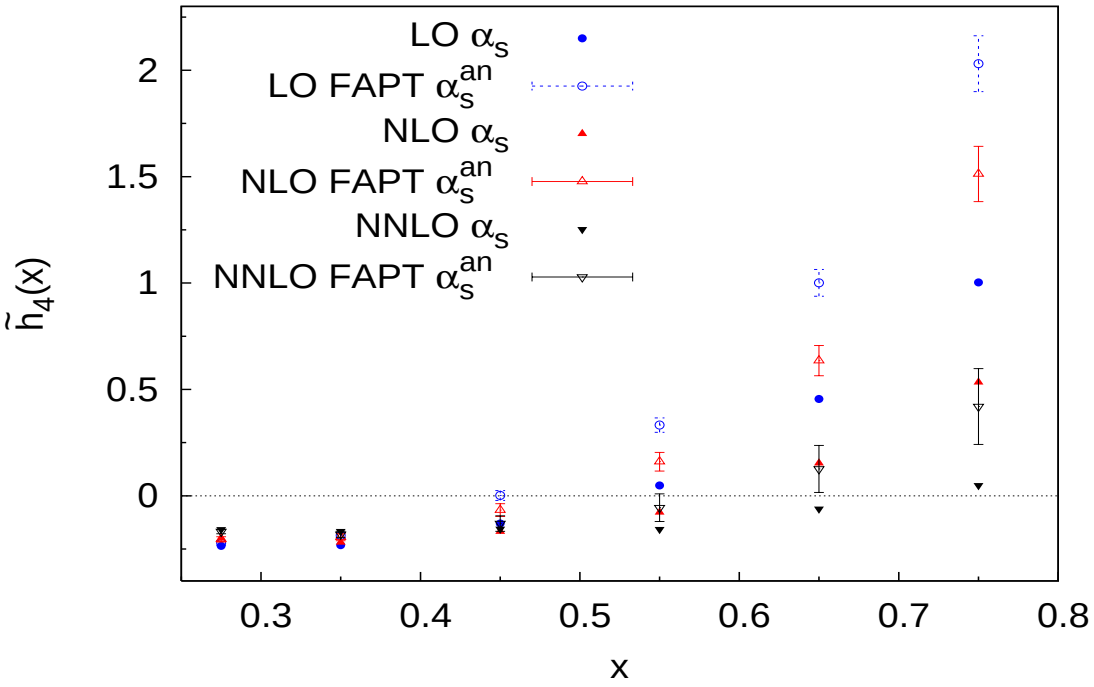


Figure 6: Comparison of the HTC parameter $\tilde{h}_4(x)$ obtained at LO, NLO and NNLO for hydrogen data within a FFNS ($n_f = 4$) between the cases with a standard perturbative and FAPT-inspired α_s.

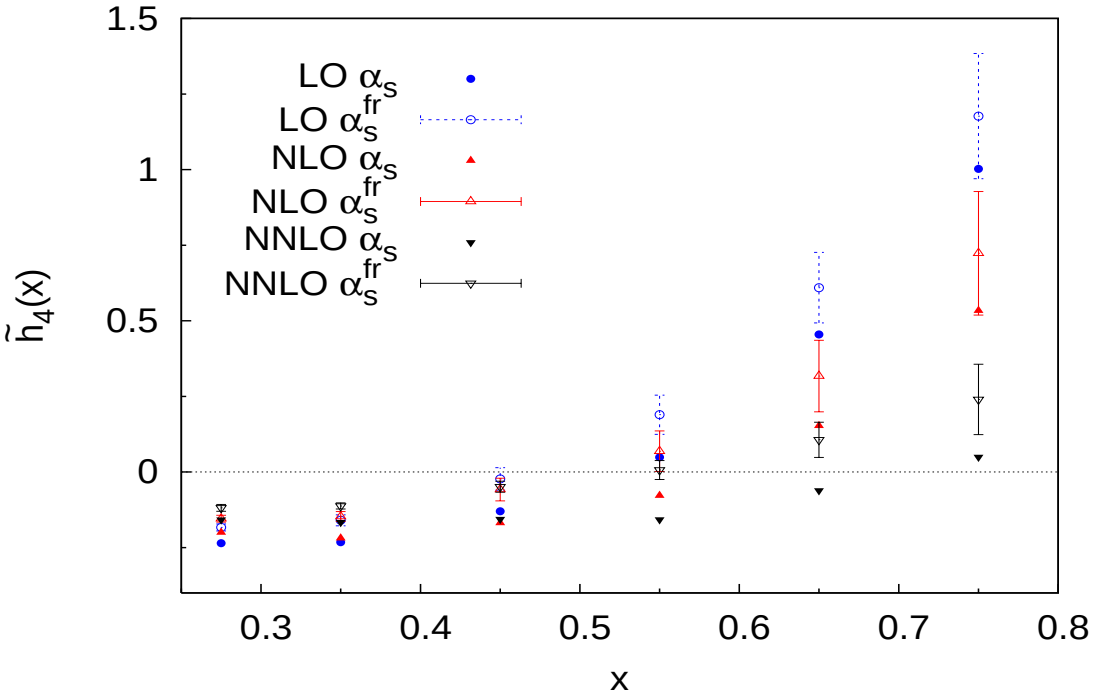


Figure 7: Comparison of the HTC parameter $\tilde{h}_4(x)$ obtained at LO, NLO and NNLO for hydrogen data within a FFNS ($n_f = 4$) between the cases with a standard perturbative and "frozen" α_s.